

AD-A023 595

KA-BAND POWER HANDLING CAPABILITIES OF SELECTED  
RADOME MATERIALS

Naval Research Laboratory  
Washington, D. C.

March 1976

DISTRIBUTED BY:

**NTIS**

National Technical Information Service  
U. S. DEPARTMENT OF COMMERCE

121107

NRL Memorandum Report 3232

# **K<sub>a</sub>-Band Power Handling Capabilities of Selected Radome Materials**

**C. J. STILLINGS**

*Satellite Communications Branch  
Communications Sciences Division*

**March 1976**



REPRODUCED BY  
**NATIONAL TECHNICAL  
INFORMATION SERVICE**  
U. S. DEPARTMENT OF COMMERCE  
SPRINGFIELD, VA. 22161

**NAVAL RESEARCH LABORATORY**  
Washington, D.C.



ADA 023595

REPORT DOCUMENTATION PAGE		READ INSTRUCTIONS BEFORE COMPLETING FORM
1 REPORT NUMBER NRL Memorandum Report 3232	2 GOVT ACCESSION NO.	3 RECIPIENT'S CATALOG NUMBER
4 TITLE (and Subtitle) K <sub>a</sub> -BAND POWER-HANDLING CAPABILITIES OF SELECTED RADOME MATERIALS		5 TYPE OF REPORT & PERIOD COVERED
		6 PERFORMING ORG REPORT NUMBER
7 AUTHOR(s) C.J. Stillings		8 CONTRACT OR GRANT NUMBER(s)
9 PERFORMING ORGANIZATION NAME AND ADDRESS Naval Research Laboratory Washington, D.C. 20375		10 PROGRAM ELEMENT, PROJECT, TASK AREA & WORK UNIT NUMBERS Problem R01-68
11 CONTROLLING OFFICE NAME AND ADDRESS Naval Electronic Systems Command Washington, D.C. 20360		12 REPORT DATE March 1976
		13 NUMBER OF PAGES 38
14 MONITORING AGENCY NAME & ADDRESS (if different from Controlling Office)		15 SECURITY CLASS. (of this report) UNCLASSIFIED
		15a DECLASSIFICATION/DOWNGRADING SCHEDULE
16 DISTRIBUTION STATEMENT (of this Report)  Approved for public release; distribution unlimited.		
17 DISTRIBUTION STATEMENT (of the abstract entered in Block 20, if different from Report)		
18 SUPPLEMENTARY NOTES		
19 KEY WORDS (Continue on reverse side if necessary and identify by block number) Radome                      Power density K <sub>a</sub> -band                      Epoxy resin LES-8                        Polystyrene resin LES-9                        Polimide resin High-power tests            Lens dielectric		
20 ABSTRACT (Continue on reverse side if necessary and identify by block number) Development of a periscope-mounted K <sub>a</sub> -band satellite communication terminal for submarine use required development of a radome to enclose the antenna subsystem. Preliminary material tests at high RF power levels indicated that common radome materials would be unusable because of the high RF power densities anticipated. Tests were conducted on several materials to determine their power-handling capabilities. Results of these tests indicate that both quartz glass with polystyrene resin and quartz glass with polyimide resin would meet RF requirements.		

## CONTENTS

INTRODUCTION	1
HIGH POWER TEST FACILITY	2
TEST CHAMBERS	2
E-GLASS/EPOXY RESIN	6
QUARTZ CLOTH/POLYSTYRENE RESIN	8
7781 GLASS CLOTH/POLYBUTADIENE RESIN	9
QUARTZ CLOTH/EPOXY RESIN	10
QUARTZ GLASS/POLYIMIDE RESIN	10
LENS DIELECTRIC	11
CONCLUSION	11
ACKNOWLEDGEMENTS	12

ACCESSION	✓
NTIS	
DTIC	
UNCLAS	
DATE	
BY	
FILE	
A	

## K<sub>a</sub>-Band Power-Handling Capabilities of Selected Radome Materials

### INTRODUCTION

The Navy is developing a K<sub>a</sub>-band satellite communication set for possible use by the Fleet Ballistic Missile (FBM) submarine fleet. The experimental configuration, the forerunner of Survivable Satellite Communication (SURVSATCOM) equipment, is being designed and fabricated in the Navy Laboratories with the Naval Electronics Laboratory Center (NELC) as lead Laboratory and the Naval Research Laboratory (NRL) and Naval Underwater Systems Center (NUSC) providing support in specific areas such as radome development and system installation. This report briefly describes a high power test facility that was developed by NRL for testing materials and components. Results of the tests on a group of proposed materials for radome use are presented. Recommendations for future program planning are presented in the conclusion.

In the initial experiment (Project Clarinet Omen) the K<sub>a</sub>-band submarine terminal will use the Lincoln Laboratory experimental satellites LES-8 and LES-9. The uplink frequencies to these satellites are in the K<sub>a</sub>-band region (~37.5GHz). The use of this frequency band required the development of miniature components, particularly for the antenna system, to be installed in the periscope assembly. The present experimental model configuration consists of a 5.25 inch diameter paraboloidal antenna mounted on a three axis pedestal. This entire antenna/pedestal and certain radio frequency (RF) electronic components are mounted as an assembly for mounting inside a radome capping the periscope.

The radome must be nearly transparent and non-lossy over the frequency band and capable of withstanding the high pressures of deep submergence. The maximum radome outside diameter must not exceed the diameter of the periscope (~7.5 inches) to permit complete retraction of the periscope into the submarine sail.

Although the selected frequency band does facilitate the development of miniature components to fit the size requirement, a challenge also arises from the high power densities experienced by the antenna, radome,

and other RF components. These power densities are significantly higher than at the lower frequencies (about 300 MHz and 8 GHz) commonly used for military satellite communications. Transmitter power of up to one kilowatt is utilized in the experimental terminal with resulting power densities of the order of  $6\text{w}/\text{cm}^2$ . (See Fig. 5).

#### HIGH POWER TEST FACILITY

Finding a dielectric material for the radome, which would withstand the high RF power densities during message transmission and testing, has been troublesome. In order to assist in the development and testing of system components such as the periscope waveguide assembly, antenna and radome assemblies, etc., NRL developed a high power test facility for determining the performance of components and materials that may be used in  $K_a$ -band systems.

Two transmitters are available to provide high RF power in the frequency band of 36.7 GHz to 38.2 GHz. The first consists of a 1.2 kW Hughes HAC II solenoid-focused traveling wave tube (TWT), power supply, and associated ancillary components. Figure 1 is a photograph of the complete high power test chamber as used with the HAC II. The second power source consists of the 1 kW high power amplifier (HPA) developed for NRL's SURVSATCOM feasibility model terminal. The latter HPA utilizes the Siemens V684, 1 kW, periodic permanent magnet (PPM) focused TWT in a HPA built by Raytheon for NRL. This power source is used with a second high power test chamber (Fig. 2). Either chamber can be used depending upon the nature of the associated metrology required.

The facility has provided test data on the following classes of components:

1. Dielectric materials (radomes, etc.).
2. Waveguide components.
3. Transmission line.
4. Antennas.

#### TEST CHAMBERS

The test chambers used in high power tests of material consist of metal containers approximately four feet high which are lined with RF absorbent material. A conical-shaped water load is positioned inside the chamber. Material to be tested is placed at the wide end of the load

and a test horn positioned above it. Sufficient space is allowed to focus the beam of an infrared thermometer spot beam on the center of the sample for recording temperature versus time and power. Cooling water is supplied to the load and provides the added advantage of allowing calorimetric monitoring during the test. A typical test chamber is shown in Fig. 3.

The primary horn used in power testing is a rectangular horn having an aperture area (A) of 63.29 cm<sup>2</sup>. Power levels (P<sub>t</sub>) into the horn quoted in this report were measured through a directional coupler at the input to the horn. Power densities at the center of the aperture are of course higher than at the edge of the aperture due to its inherent cosine-square power taper. The power density (P<sub>d</sub>) at the aperture center of this rectangular horn is twice the average power density; so

$$P_d = 2 \frac{P_t}{A} = 0.3160 P_t \frac{\text{watts}}{\text{cm}^2}$$

In all cases, the measured power densities in this report are at the center of the rectangular horn being used.

In order to determine the validity of tests conducted with the test horn at expected system power levels, it was necessary to analyze the power density of the candidate antenna. The relatively small area of the antenna required for use in the SURVSATCOM terminal (5.25 inch diameter) results in high power densities at the center of the aperture. The expected transmission line loss from the 1000 watt transmitter is 6 dB in the experimental model of the system. The maximum power input to the antenna would be 251 watts. The power density is calculated for the paraboloidal antenna having an aperture area of 140 cm<sup>2</sup> (5.25 inch diameter).

The antenna manufacturer states that the illumination characteristic of this antenna is between a cos<sup>3</sup> and cos<sup>2</sup> function and exhibits a 20 dB taper. Since no more detailed information was available, the analysis was performed for both a cos<sup>3</sup> and a cos<sup>2</sup> illumination.

An antenna with cos<sup>n</sup> power distribution function and taper is as shown in Fig. 4. The power density is computed as follows:

For a circular aperture with a  $\cos^n$  illumination the total power ( $P_t$ ) is given by

$$P_t = \int_A p(r) dA$$

where  $dA$  is an annular element of area given by

$$dA = 2 \pi r dr$$

in which  $r$  is the distance from the center of the aperture and  $dr$  is the width of the annulus. The power distribution function  $p(r)$  across the aperture is given by

$$p(r) = C \left\{ \cos^n \left( \frac{r}{R} \frac{\pi}{2} \right) + B \right\}$$

where  $C$  and  $B$  are constants determined by the total power and the taper.

The power density  $p(0)$  at the center of the aperture is

$$p(0) = C(1 + B).$$

Therefore to determine  $p(0)$ ,  $C$  and  $B$  must be determined. By definition of the taper ( $t$ ),

$$t = \frac{p(R)}{p(0)} = \frac{B}{1 + B}$$

where  $R$  is the radius of the aperture. Solving for  $B$ ,

$$B = \frac{t}{1-t}$$

making

$$P_t = 2 \pi C \int_0^R \left\{ \cos^n \left( \frac{r}{R} \frac{\pi}{2} \right) + B \right\} r dr$$

and

$$C = \frac{P_t}{2 \pi \int_0^R \left\{ \cos^n \left( \frac{r}{R} \frac{\pi}{2} \right) + B \right\} r dr.}$$



To determine  $p(0)$

$$p(0) = C (1 + B) = C \left( \frac{1}{1 + t} \right) \frac{P_t}{(1 - t) 2 \pi \int_0^R \left\{ \cos^n \left( \frac{r}{R} \frac{\pi}{2} \right) + B \right\} r dr} .$$

When  $n = 2$

$$p(0) \Big|_{n=2} = \frac{P_t}{\pi R^2 \left\{ t + \left( \frac{1}{2} - \frac{2}{\pi^2} \right) (1-t) \right\}}$$

and for a 20 dB taper ( $t = 0.01$ ) and an aperture of  $140 \text{ cm}^2$

$$p(0) \Big|_{n=2} = 0.02347 P_t \frac{\text{watts}}{\text{cm}^2} .$$

When  $n = 3$

$$p(0) \Big|_{n=3} = \frac{P_t}{\pi R^2 \left\{ t + \frac{8}{3\pi} - \frac{52}{9\pi^2} (1-t) \right\}}$$

and for a 20 dB taper ( $t = 0.01$ ) and an aperture of  $140 \text{ cm}^2$

$$p(0) \Big|_{n=3} = 0.02638 P_t .$$

Figure 5 uses these numbers to show the relationship between input power and power density for the various antennas.

## E-GLASS/EPOXY RESIN

The initial selection of a material for use with the NRL feasibility demonstration model SURVSATCOM terminal was accomplished in cooperation with NUSC. A material was selected which was known to have good mechanical properties. This choice, (E-glass/epoxy resin), was predicated on the success of previous radomes for submarine use and not on its power handling capability. The initial material thickness was determined by computing the strength required to meet the pressure specification. Once the dielectric constant ( $\epsilon$ ) and loss tangent ( $\delta$ ) were determined experimentally at NRL by measurement of a sample, the initial thickness was increased to the nearest half wavelength ( $3 \lambda/2$  in this instance) to minimize transmission loss. This still resulted in a lossy radome ( $\sim 1$  dB), but sufficient power was available to overcome the loss; therefore, emphasis was placed on the mechanical aspects of radome design. Mechanical tests performed by NUSC in a pressure tank indicated that the radome would withstand pressures up to 2500 PSI. The high loss, however, posed a heating problem due to the power dissipated and the relatively poor thermal conductivity of the material. To determine the extent of this problem, samples of the material lay-up were obtained and subjected to RF power testing. Initial tests at maximum power determined almost instantly that the material would not withstand the high power density expected. Due to scheduling difficulties, this first test was performed with a smaller rectangular test horn having an area of  $9.3 \text{ cm}^2$ . Total power applied to the horn was 75 watts, resulting in a power density of  $16 \text{ w/cm}^2$ \* at the center of the aperture. The duration of the test was five minutes. The result of this test was extensive charring of the material (see Fig. 6).

To further determine the power density which the material could safely withstand, three additional tests were conducted. The first two tests required no additional instrumentation other than a video tape system and were intended to determine if the material could withstand power densities of  $1 \text{ w/cm}^2$  and  $5 \text{ w/cm}^2$ . RF power corresponding to  $1 \text{ w/cm}^2$  (32 watts) was applied to the primary test horn (area  $63.29 \text{ cm}^2$ ) which was now available. The test was continued until discoloration could be detected by the video camera. In this case discoloration occurred after 5 minutes. A new sample was inserted into the test fixture and the power

---

\*This power density exceeds  $6 \text{ w/cm}^2$  maximum expected from the terminal.

density set to  $5 \text{ w/cm}^2$  (155 watts). The results of this test were as follows: After 60 seconds discoloration could be detected. After 90 seconds the material began to smoke. Blistering occurred after 110 seconds had elapsed with the material exploding in flames after a duration of 130 seconds. Figure 7 shows the extent of the damage. The center portion of the area under radiation bubbled and separated from the laminate thereby reducing the effect of charring in this area. The effect can be seen at the edges, however. Evaluation of these tests indicated that the contrast resolution of the video system was not fine enough to detect the first signs of discoloration so that no conclusive information could be obtained as to when the damage actually began.

The third test provided very definitive information. A section of the radome was placed in the chamber and RF power was applied for a period of 15 minutes at each of five different power levels from 10 watts ( $0.316 \text{ w/cm}^2$ ) to 50 watts ( $1.58 \text{ w/cm}^2$ ) in 10 watt increments. An infrared thermometer was placed inside the chamber with the sensor aimed at the center of the sample under the horn. The thermometer was connected to a chart recorder to record the increase in temperature with time. After each fifteen minute period the sample was immediately removed and immediately placed (so that no significant cooling could occur) in a test fixture (see Fig. 8) on the mechanical X drive of an X/Y plotter. An external voltage was applied to the X axis electrical drive to create a slow linear scan. An infrared thermometer was located such that the material would pass directly through the sensor spot at the location corresponding to the area directly under the center of the horn. The output of the thermometer was then instrumented to the Y axis to record temperature across the surface area. After each recording, the sample was permitted to cool before being returned to the chamber. Results of this test can be seen in Figure 9.

The test indicated that the material could probably withstand power densities up to approximately  $0.95 \text{ watts/cm}^2$  without delaminating because no discoloration was evident at this power level. However, this exposure was for a period of only fifteen minutes and the temperature of the material was still increasing at that time so that no absolute conclusion should be drawn from this data. Also after a duration of fifteen minutes at a power density of  $1.5 \text{ watts/cm}^2$  the material reaches the temperatures at which the resin was cured ( $\sim 300^\circ\text{F}$ ).

Recently another material sample in this same category was submitted for power testing. This material (E-glass/E293 Epoxy resin) was

subjected to the same tests as for previous samples. As expected, the material exhibited characteristics similar to those in this category already tested. The results of this test are presented in Figures 10 and 11.

#### QUARTZ CLOTH/POLYSTYRENE RESIN

Failure of the initial radome material was the catalyst for a search for better materials. NRL had contracted with the Radiation Division of Harris Intertype Corp. to produce a pedestal for the NRL feasibility model demonstration. Included in this procurement was a thermal analysis of the antenna system. Since the radome was an important part of this analysis, Radiation, Inc. analyzed the material and independently determined that the E-glass/Epoxy combination would not meet the requirements, and proposed to use a material (quartz cloth and modified polystyrene resin) with which they had had extensive experience. NRL agreed to fund the fabrication of a radome subject to successful power testing of the material. Samples were submitted for testing and the results were encouraging. This combination withstood a power density of 25 watts/cm<sup>2</sup> for a period of one hour with almost no perceptible damage. Figure 12 is a photograph of the material after exposure. Temperature plots of the material were made for various input power densities. The photograph and the data in Figure 13 indicates that this material will withstand more than the maximum expected antenna power density of approximately 6 watts/cm<sup>2</sup> (25 watts at the antenna). At this point the measured temperature of the material approached 160°F, well below the curing temperature (~300°F) of the resin.

The results of this test provided enough confidence to commission the fabrication of two radomes. The first radomes were laid up in a vacuum bag and were not of good mechanical quality. Cracks and air pockets were visible throughout, giving the impression that the mechanical strength of the radome would be insufficient to meet system requirements. To determine the radome loss, dielectric constant ( $\epsilon$ ) and loss tangent ( $\tan \delta$ ) measurements were made through both the spherical and cylindrical portions of the radome. The maximum measured loss was 0.2 dB as measured on the NRL test bench.

One radome was then shipped to the NUSC for pressure testing, in spite of the poor quality, so that information could be obtained on its mechanical properties. As expected, the radome failed at a relatively low pressure (~750 PSI). The manufacturer then improved the fabrication technique and developed a technique for laying-up the polystyrene resin

in an autoclave. The result was a radome of better mechanical properties.

This radome has been pressure tested at lower pressures (750 PSI). Data obtained from strain gauges fastened to the radome were used to extrapolate to higher pressures. This was necessary because testing-to-destruction would have left the NRL feasibility model with only one of the inferior radomes. Extrapolation from the strain gauge data indicated that the radome would withstand 1500 PSI. One of the original inferior radomes has been installed on the NRL feasibility model terminal and has been operated at power densities of  $6.5 \text{ w/cm}^2$  intermittently over a period of several months (for periods of several hours each) with no discernible damage. However, due to the original fabrication cracks on the inner surface of the radome, photographic records will be made of the inner surface both before and after further tests before definite conclusions will be reached. No evidence of charring has been observed.

#### 7781 GLASS CLOTH/POLYBUTADIENE RESIN

In order to insure a selection of suitable materials for use in radome fabrication, power tests were performed on several other material samples. Two of these samples fall in the same category, Type 326 Dienite/7781, and Type U341 style 7781.

Figure 14 is a plot of temperature versus sample area for a sample of Type 326/7781 Dienite taken after being subjected to a power density of  $10 \text{ w/cm}^2$  for a duration of 4 minutes. The material reached a temperature of  $500^\circ\text{F}$  and charred badly (see Fig. 15).

Figure 16 shows similar data for a sample of Type U341 style 7781 for power densities of 1.6, 2.2 and  $3.2 \text{ w/cm}^2$  for a period of 15 minutes each. This material reached a temperature exceeding  $250^\circ\text{F}$  for a power density of  $2.2 \text{ w/cm}^2$  and exhibited characteristics similar to those of the E-Glass and 7781 Epoxy resin samples described previously. Use of this material is clearly not recommended.

The test for the 326/7781 Dienite was an earlier test and was conducted to determine only if the material could handle the peak power densities expected at that time. Attempts were made to obtain additional samples for testing at lower power densities but those attempts were unsuccessful. It is doubtful, after evaluating the data, that this material would exhibit better properties than Type U341 style 7781.

#### QUARTZ CLOTH/EPOXY RESIN

The NELC feasibility model radome is fabricated of quartz and epoxy resin by CHU Associates. The radome was originally expected to operate with an estimated maximum antenna input power of 70 watts ( $1.8 \text{ w/cm}^2$ ) for a 250 watt HPA. With the selection of the 1 kW design the maximum input power is expected to be approximately 250 watts ( $6.4 \text{ w/cm}^2$ ). The system will not be operated at this level often, and due to built in power control, it can be assumed that the maximum power density this radome would experience is  $3.2 \text{ w/cm}^2$ . To determine the ability of this composite to withstand this power density, tests were performed as for previous material samples, plotting temperature versus time at various power densities. Figure 17 shows the temperature versus time characteristics of the tested sample. Temperatures were measured as close to the center of the aperture as possible. Due to the shape of the sample and the space limitations of the test chamber, it was not possible to reach the center with the infrared thermometer, and the temperatures recorded are at least ten percent lower than the temperatures measured with the X/Y plotter (Fig. 18). Temperatures shown in Figure 18 were measured at the hottest spot of the sample. Data shown in Figure 17 is useful in predicting the temperature rise with time as a function of power for this material. The material showed no external signs of scorching until the power density reached a level of  $2.2 \text{ w/cm}^2$  where the temperature exceeded  $300^\circ\text{F}$ . However, at a power density of  $1.5 \text{ w/cm}^2$  an odor of burning resin began to emanate from the test chamber. It is clear that this material has limitations and will not handle the expected power density of the system. Use of this material for this intended application is not recommended. If a decision were made to use this material, it should be used cautiously, taking care to absolutely limit the maximum operating power density to a level of less than  $1 \text{ w/cm}^2$ . This will limit the system transmit capability if the system is required to transmit for long periods. Any damage to the resin will probably be accumulative and will affect the mechanical properties of the radome as well, resulting in severe system damage (antenna damage by water due to radome failure) even at reduced pressures.

#### QUARTZ GLASS/POLYIMIDE RESIN

The very latest material tested has so far shown good promise of meeting most of the system operating requirements. This material (Quartz Glass/Polyimide Resin) has withstood power densities of  $25 \text{ w/cm}^2$  with no apparent damage. Results of the tests on this material

are shown in Figures 19 and 20. Figure 19 shows the temperature versus power versus time characteristics. Figure 20 shows the temperature versus power across the surface of the material.

This material has withstood high power densities better than any other with the exception of quartz/polystyrene. This material has shown greater mechanical strength than quartz/polystyrene in tests conducted at NUSC. The sample tested was extremely porous and will present serious problems due to water absorption. This problem remains to be solved and ultimately may limit its use. This problem warrants further study since mechanical analysis of these materials was beyond the scope of this study.

#### LENS DIELECTRIC

The NRL SURVSATCOM feasibility model antenna consists of a lens corrected corrugated horn assembly having a diameter of 4 inches. The original lens was fabricated of Emerson and Cummings HT-003 teflon material. To facilitate use of HT-003 teflon, which is manufactured in the form of beads, it was combined with a binding resin. The lens is located directly in the field of the horn and is subjected to a high power density particularly at its apex. To determine the ability of the material to withstand the maximum power expected, RF power testing was conducted.

The test was conducted with the lens in its normal position inside the horn. RF power was applied with the horn positioned above the water load.

RF power of 250 watts at a frequency of 37.4 GHz was applied continuously for a period of 20 minutes. At the end of this period, the lens was removed and visually inspected for damage. Figures 21 and 22 show the extensive charring which occurred. This material is obviously unsatisfactory for this application and a new material was sought.

Experiments proved that both machined solid teflon and fused silica would handle the high power densities experienced by the lens. Of these two candidates teflon was chosen for its ease of fabrication and its non-brittle characteristic. The resulting lens has been in use successfully for a period of two years with no resulting damage.

#### CONCLUSION

Data provided in this report was obtained during tests of candidate



materials designed for specific applications. To date no material sample has been successfully tested which would satisfy the radome application completely. A composite of quartz glass and polystyrene resin provides the best RF and thermal characteristics but will not meet the maximum mechanical requirement without further development. The remaining materials tested met only the mechanical requirements as shown by NUSC, but do not meet the RF requirements with the exception of Quartz/Polyimide, which tends to be very porous. This porosity leads to problems with water absorption which presents RF loss problems and ultimately leads to destruction when the absorbed moisture begins to heat. More material development and testing is required in the search for a successful candidate for use in this radome application. If mechanical specifications cannot be relaxed, a shotgun development of new materials or fabrication techniques which would successfully meet all requirements should be initiated. Serious delays in the program will be experienced unless a decision is made and a more extensive search is made of available materials.

Reducing the RF requirements for the radome has been considered. Power levels should be reduced where possible, but it is unwise to depend on power control circuits to protect the radome. The correct approach is to design the radome to meet the maximum possible exposures so that in the event of control circuit's malfunction, the radome will not be destroyed causing drastic damage to the antenna and associated RF components. In addition, the effects of high power on some materials may be accumulative, which could result in severe damage even at reduced power levels. The expense of radome development would be small by comparison to the possible damage. The extent of accumulative damage should be investigated in further studies.

High ambient temperatures will cause additional problems. The data presented in this report regarding temperature rise with power density and time are relative. If the ambient temperature is high, the temperature of the illuminated radome will be correspondingly higher. The system for which the radome is being designed will exhibit high ambient temperatures caused by heat dissipation from system components and the environment (including solar radiation).

#### ACKNOWLEDGEMENTS

Grateful appreciation is extended to Mr. Richard Gariazzo of NUSC for his assistance in acquiring radome samples, Mr. John Ayoub for his



assistance in low power measurement of material characteristics, and Mr. Raymond Cushing for his assistance in high power tests of the materials covered in this report. In addition, appreciation is extended to the NRL Engineering Services Division for their assistance in fabrication of the water loads used extensively in this study.

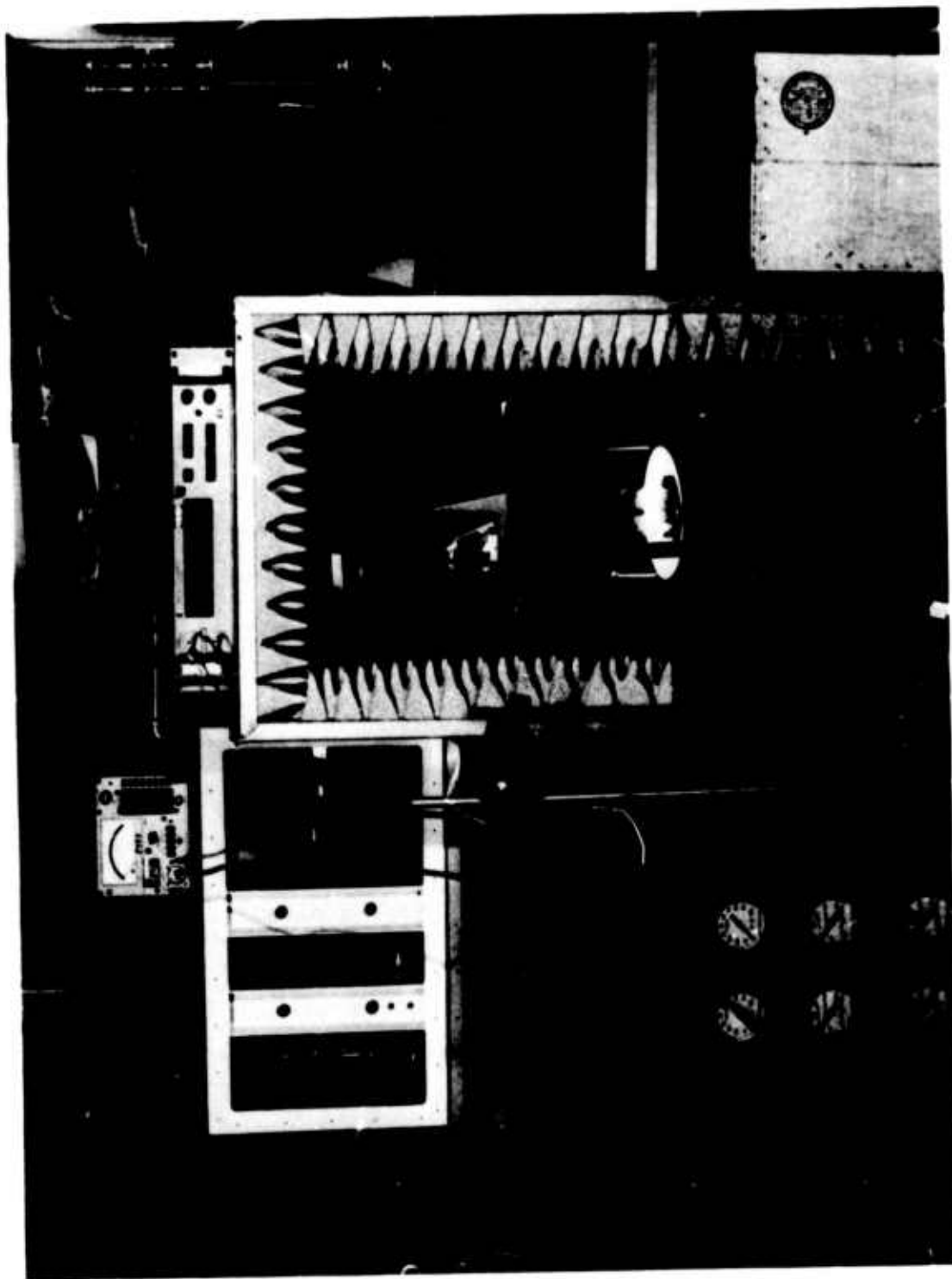


Fig. 1 — High-power test facility with Hughes HAD II traveling-wave tube

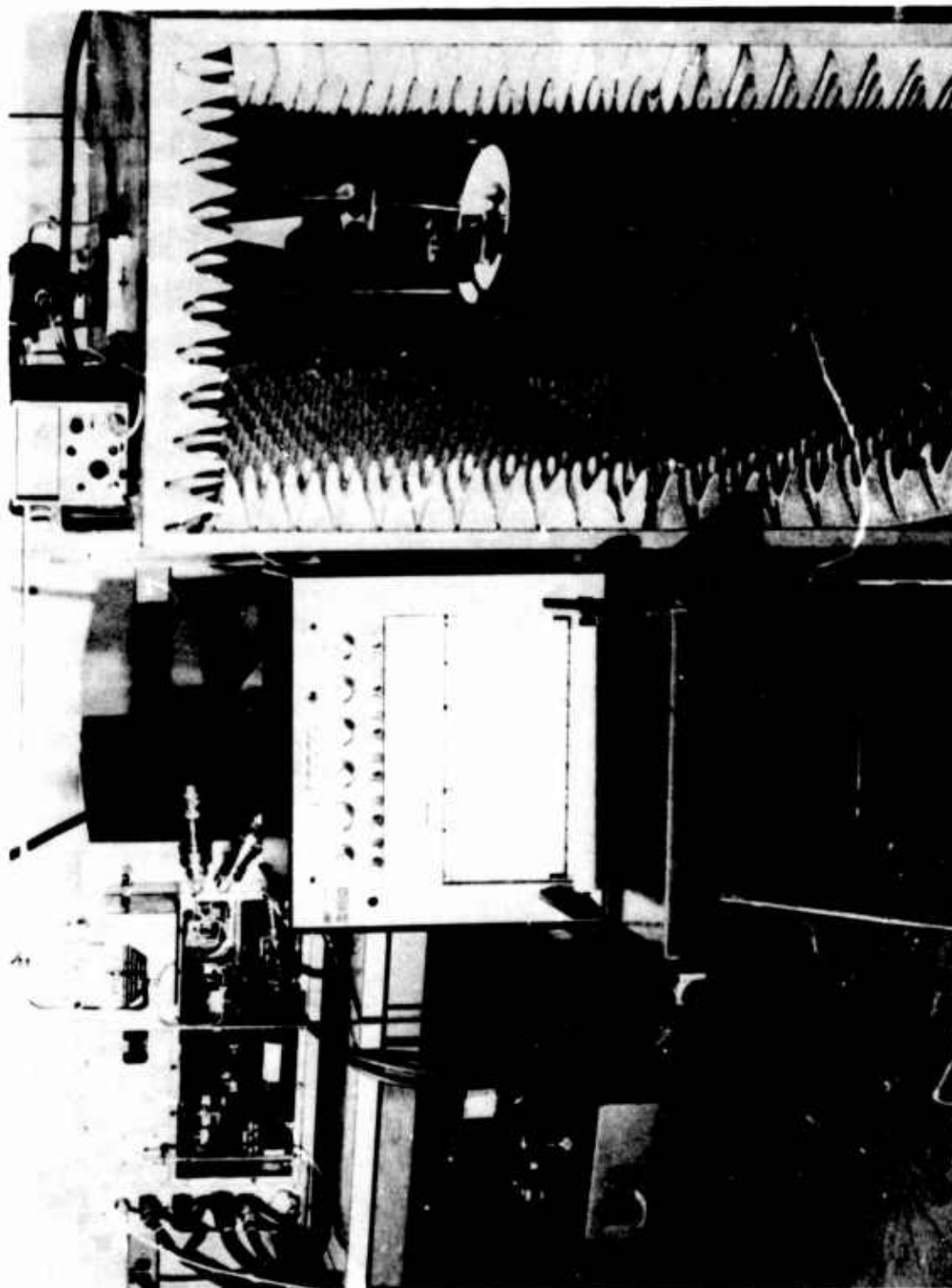


Fig. 2 — High-power test facility with Raytheon high-power amplifier



Fig. 3 — Typical K<sub>a</sub>-band high-power test chamber

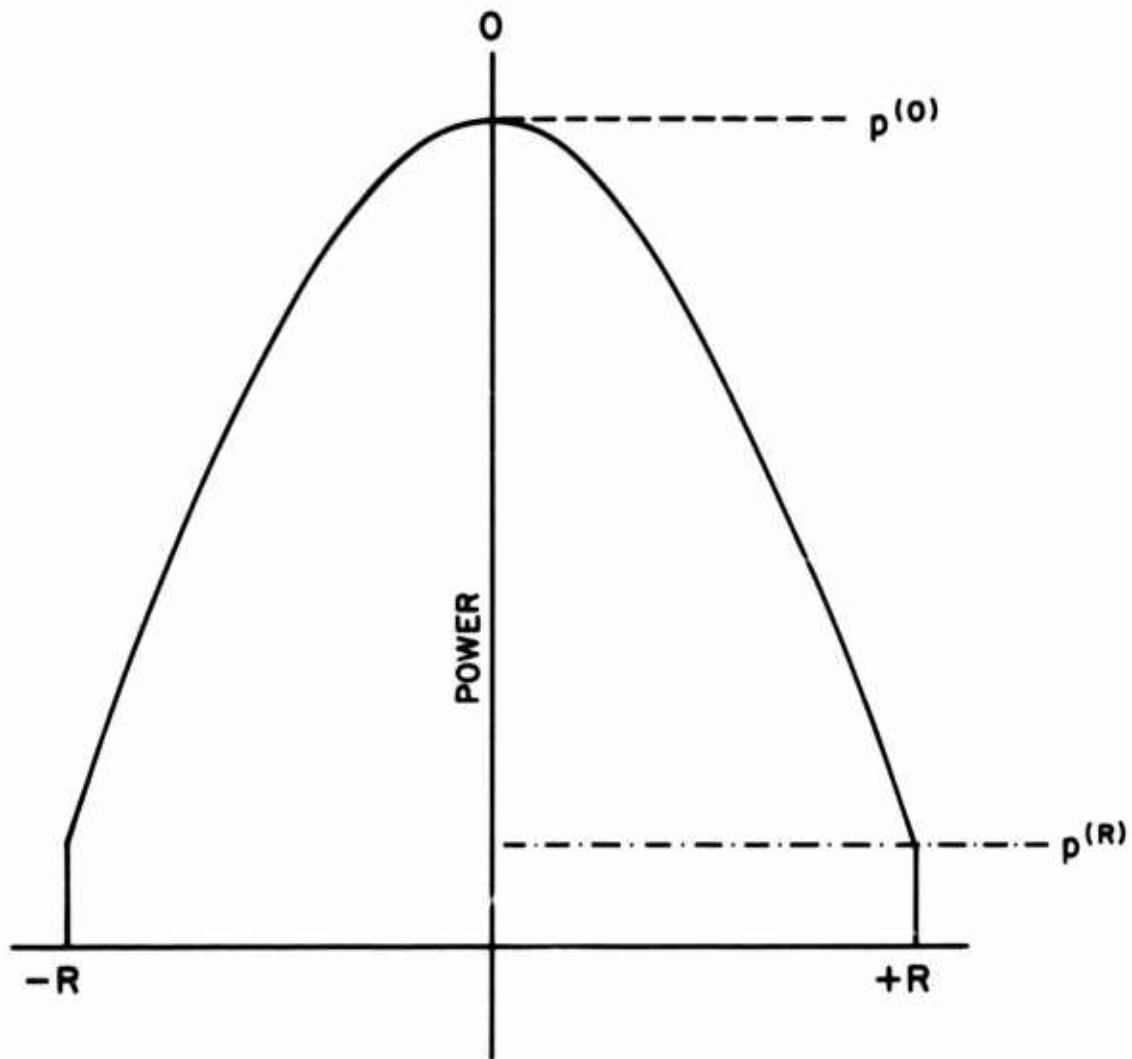


Fig. 4 — Truncated  $\cos^n$  power distribution taper

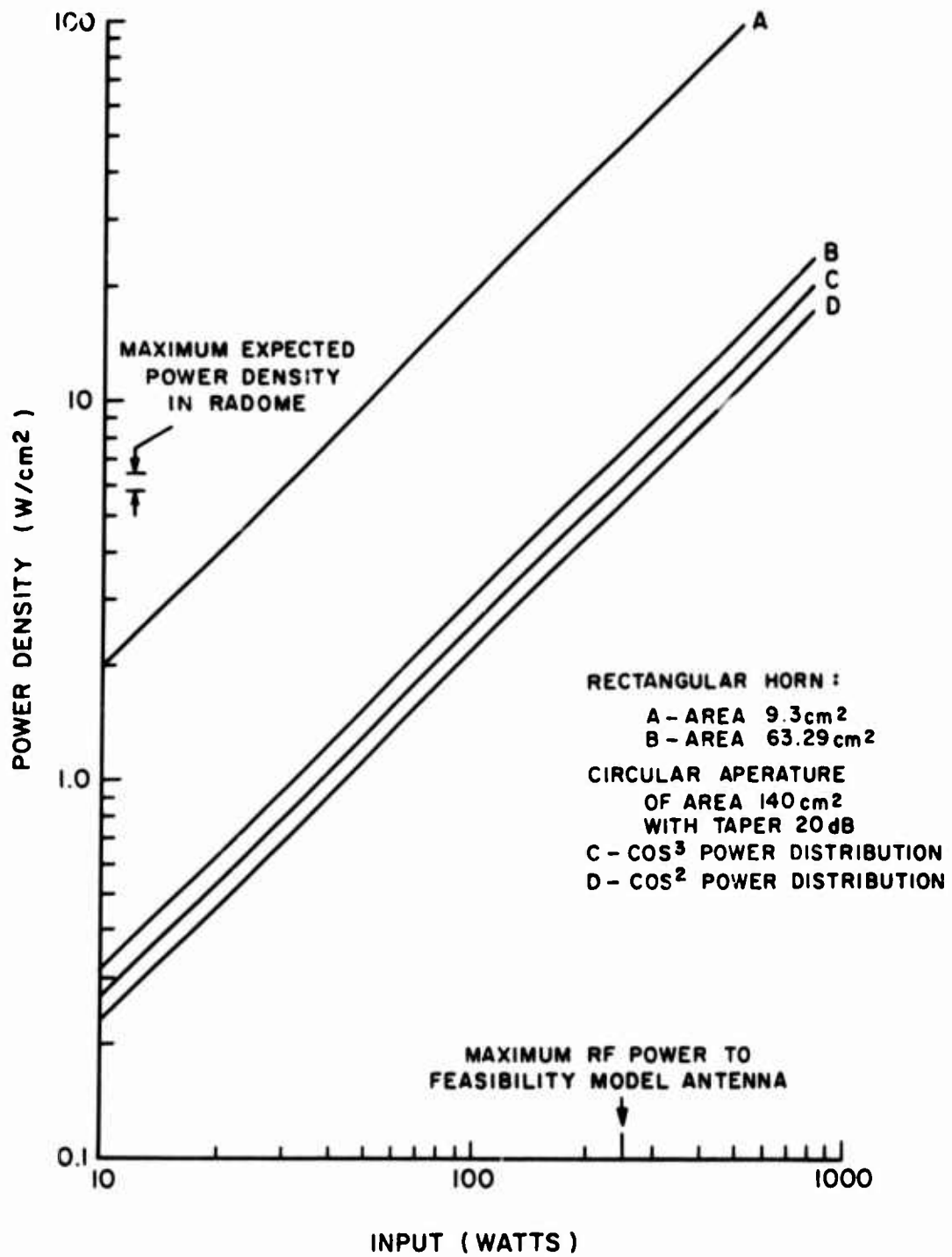


Fig. 5 — Power density vs input power for selected antennas



Fig. 6 -- E-glass/epoxy resin sample after initial test

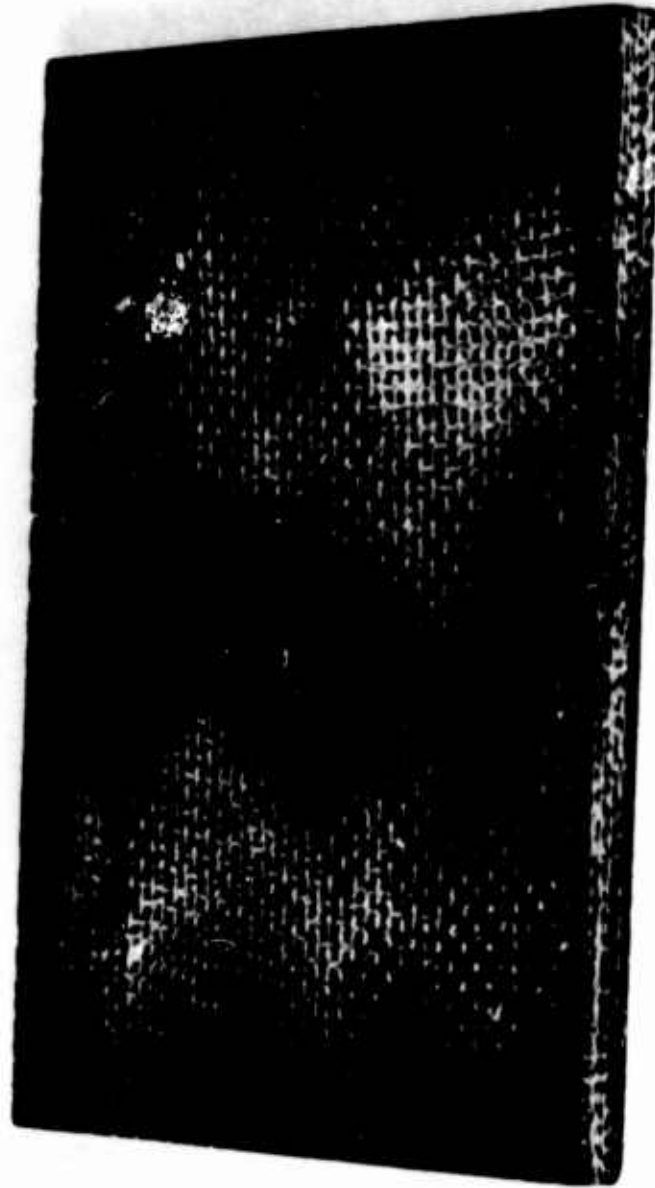
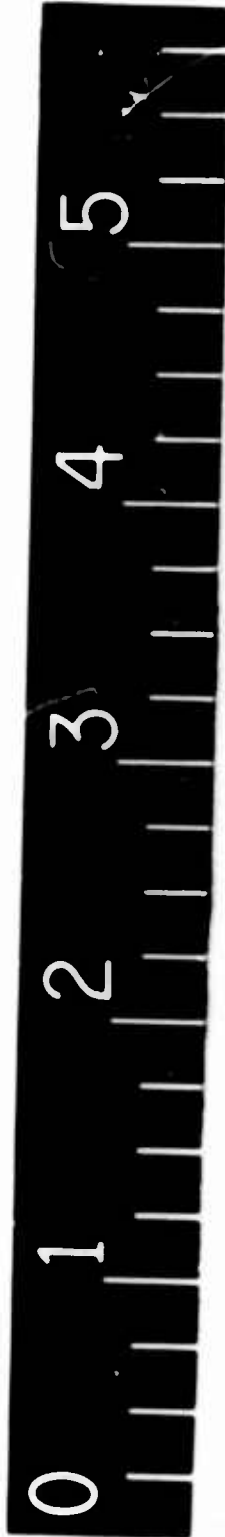


Fig. 7 — E-glass/epoxy resin sample after 130 seconds (Test 2)



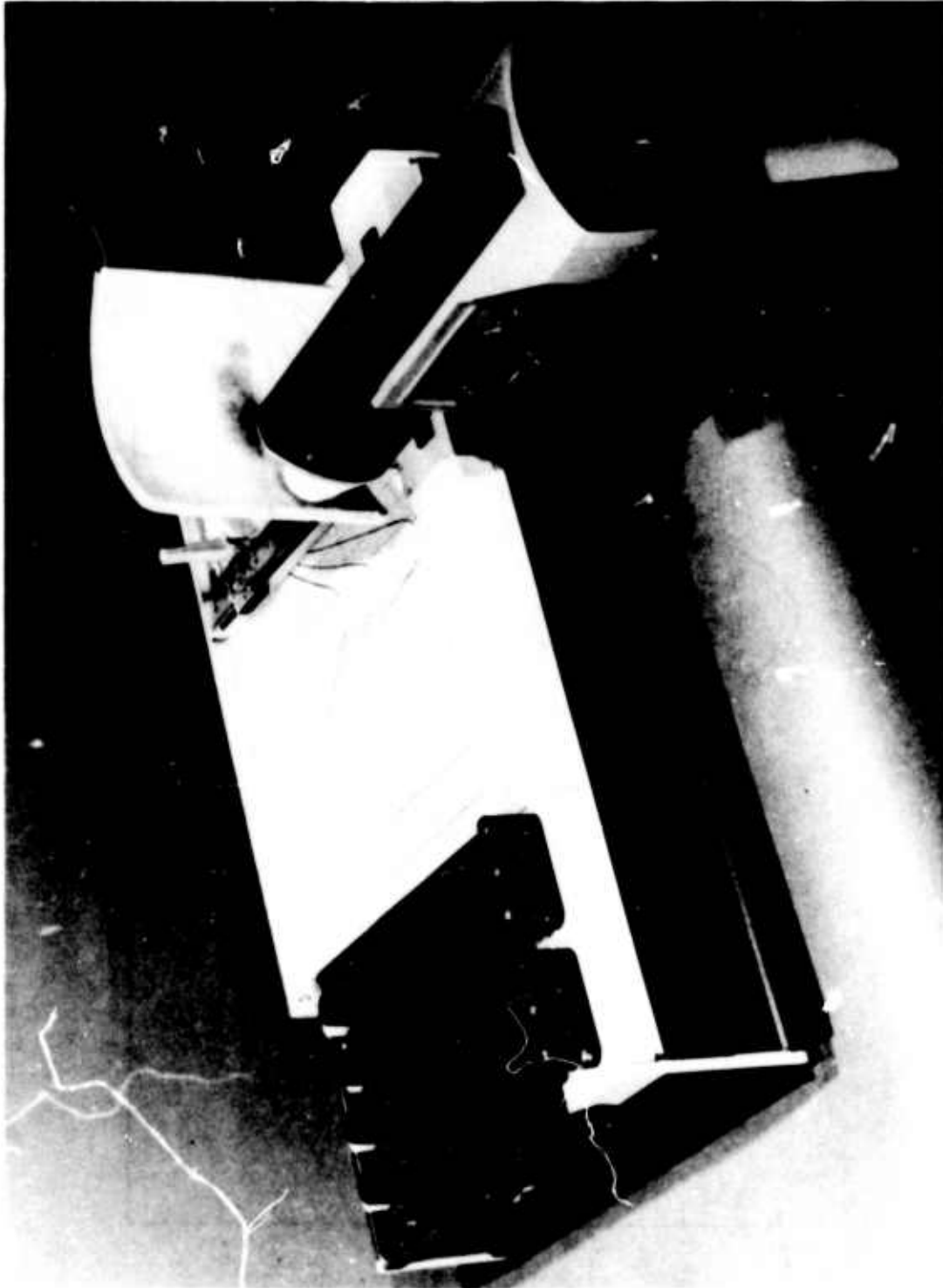


Fig. 8 — Infrared-temperature-measuring test fixture

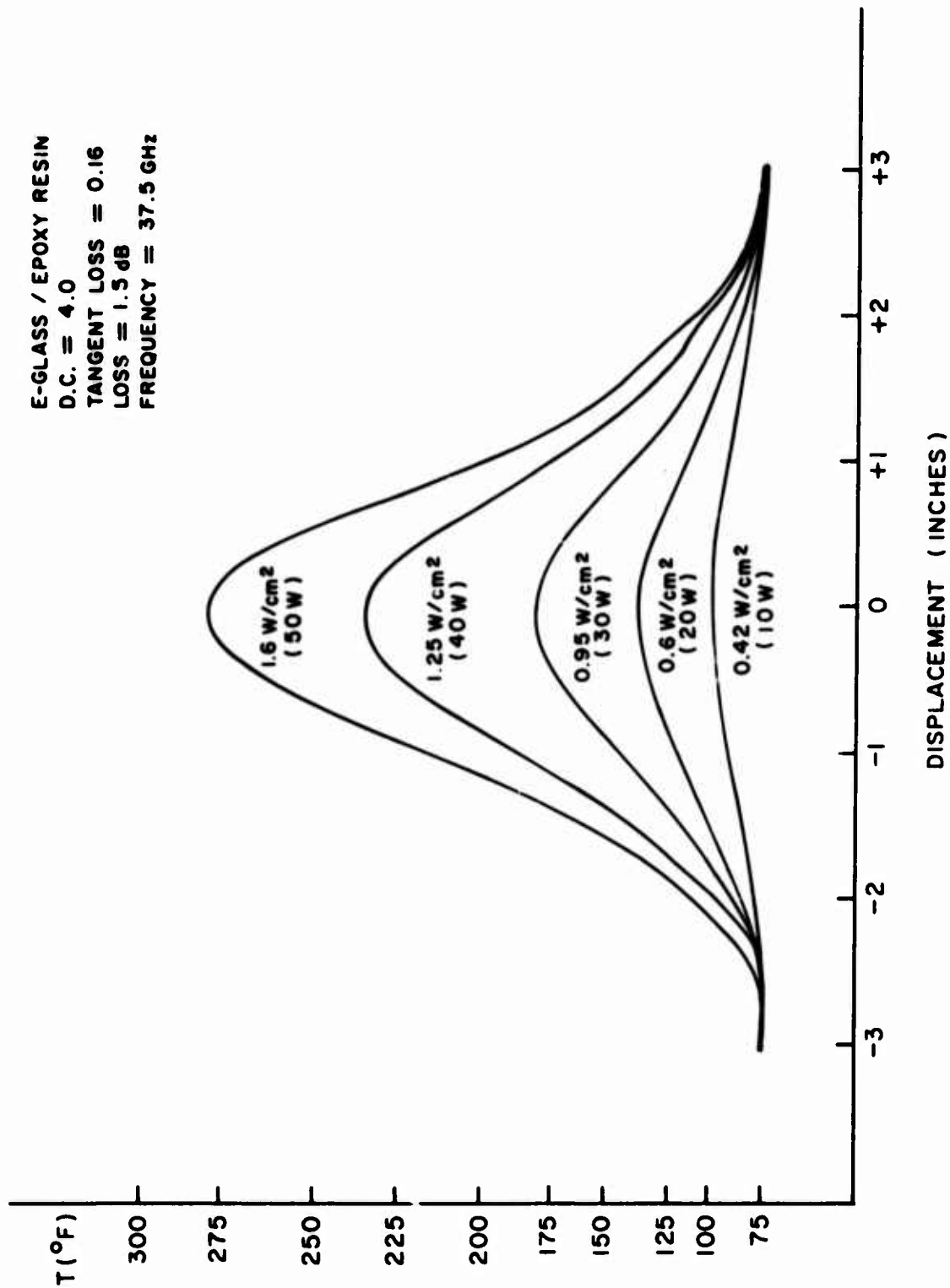


Fig. 9 — E-glass/epoxy resin temperature as a function of power density and displacement

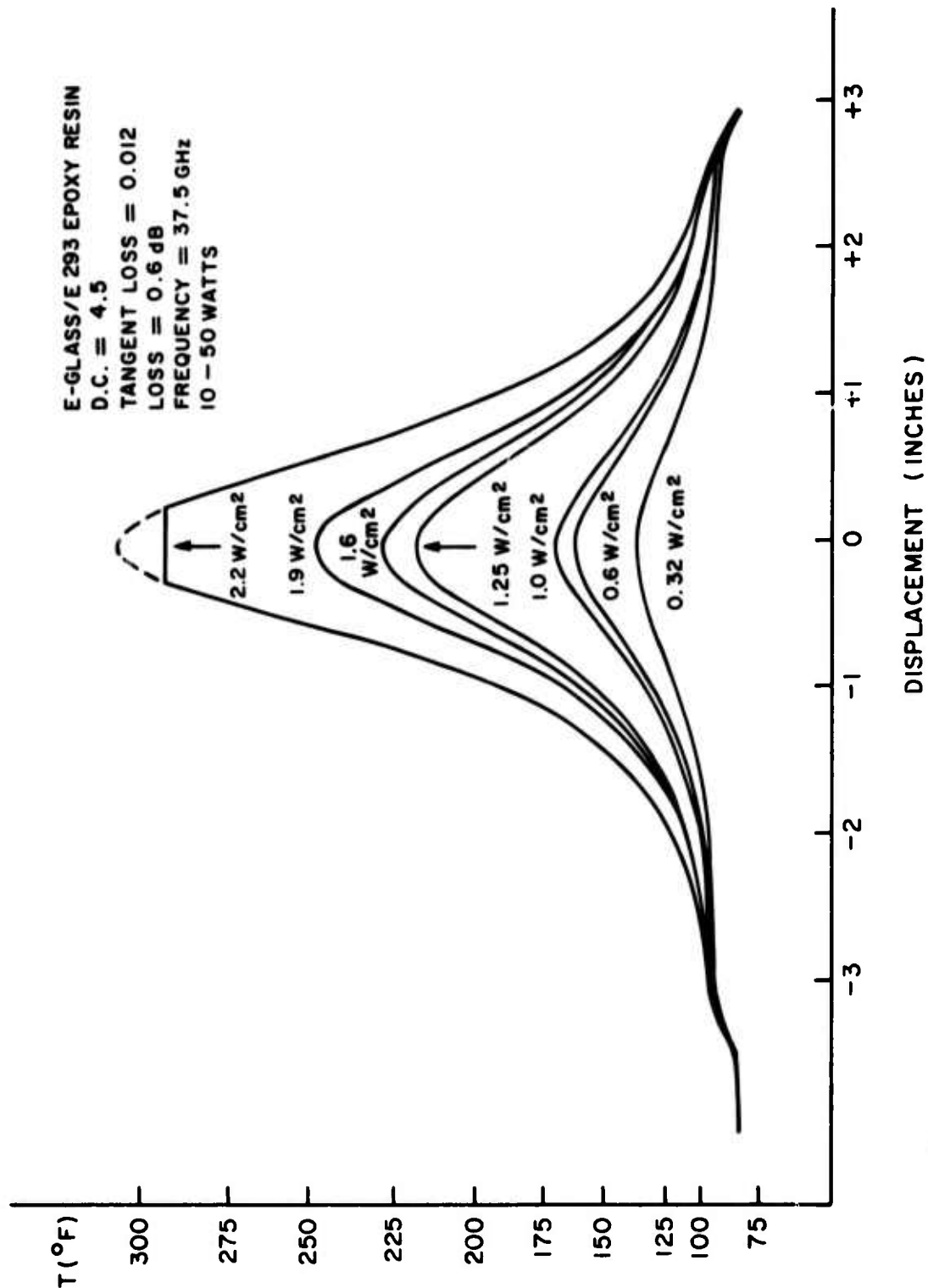


Fig. 10 — E-glass/E293 resin temperature as a function of power density and displacement

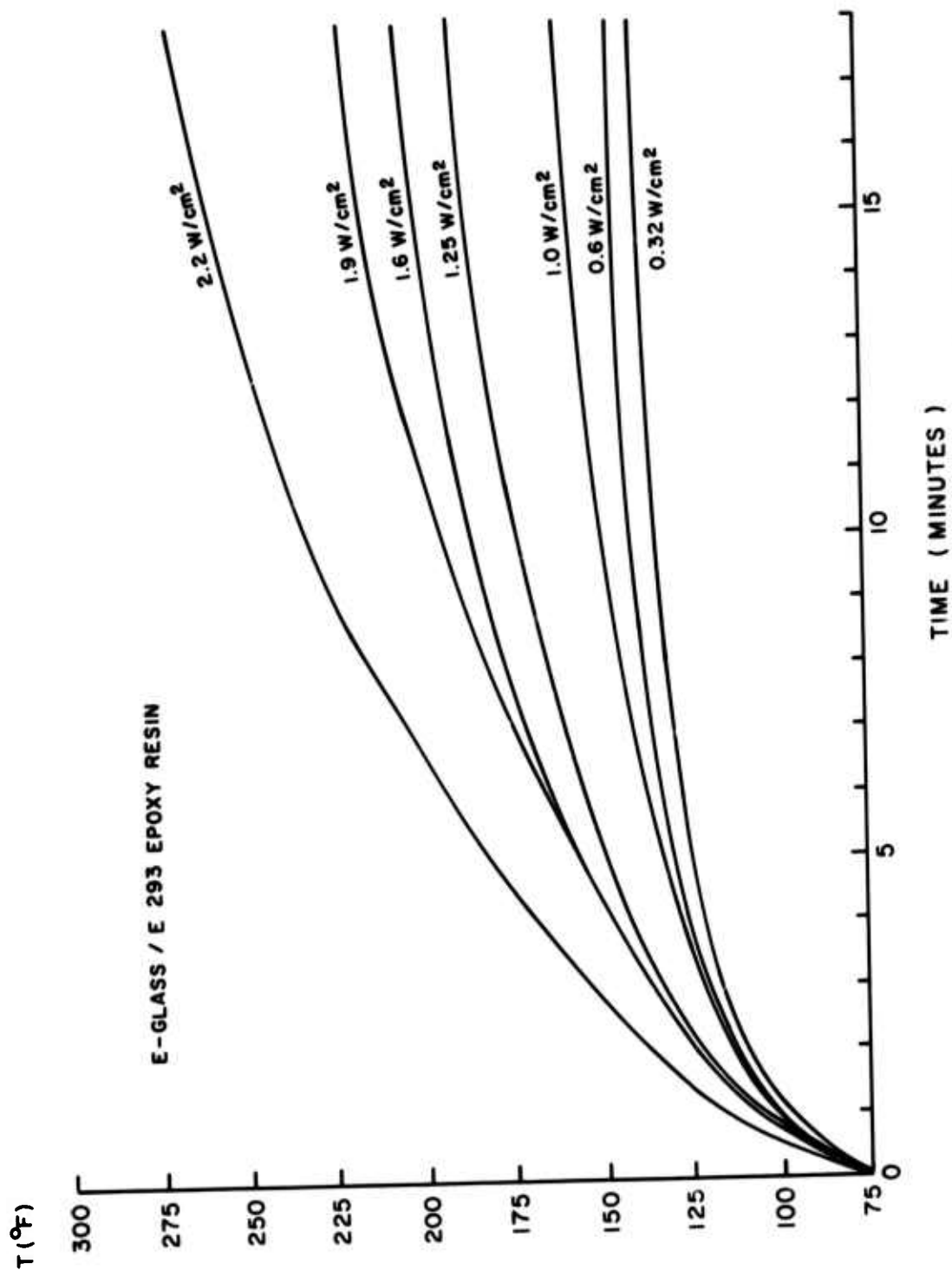


Fig. 11 — E-glass/E293 resin temperature as a function of power density and time

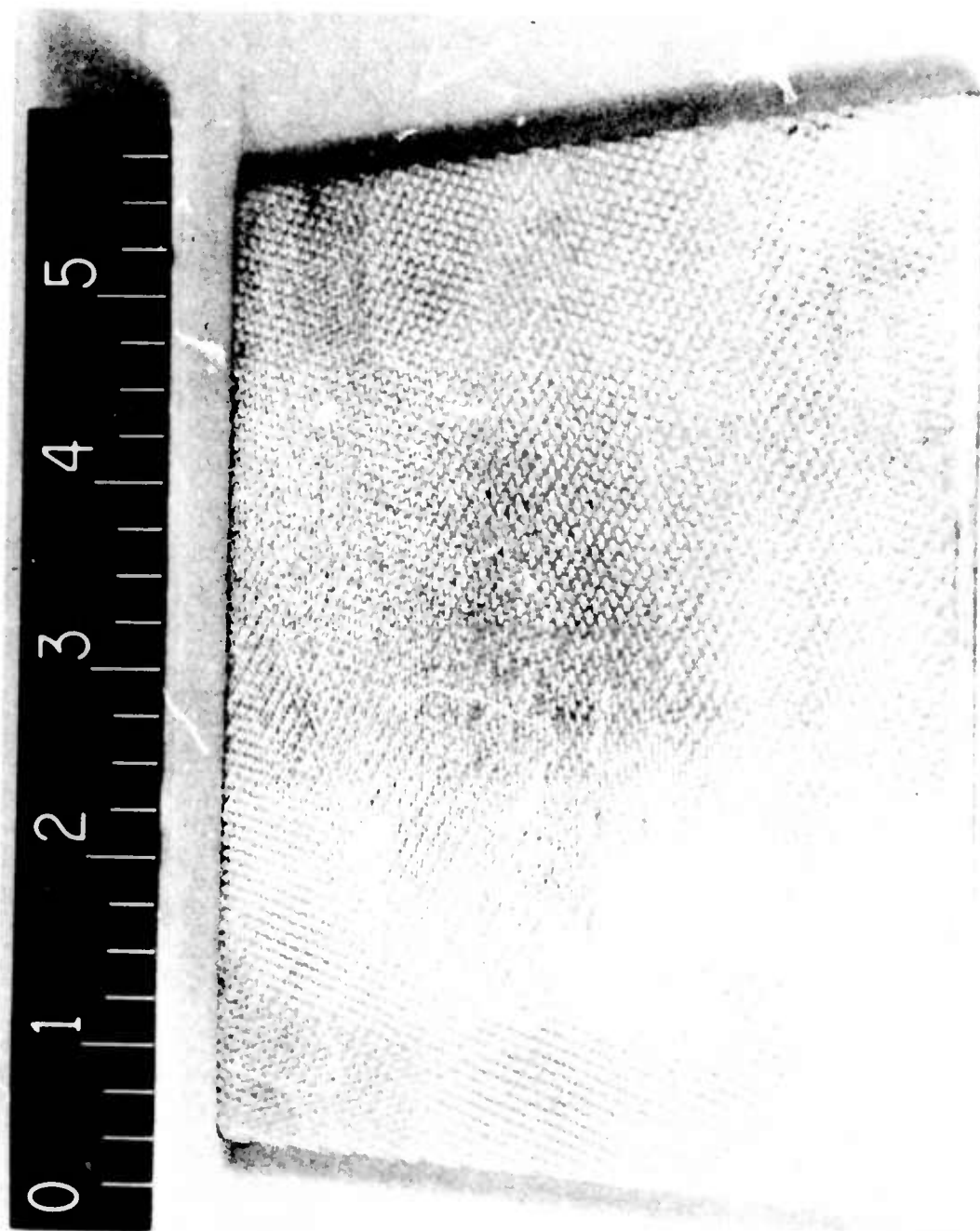


Fig. 12 — Quartz cloth/polystyrene resin after exposure to  $25\text{W}/\text{cm}^2$  for 1 hour

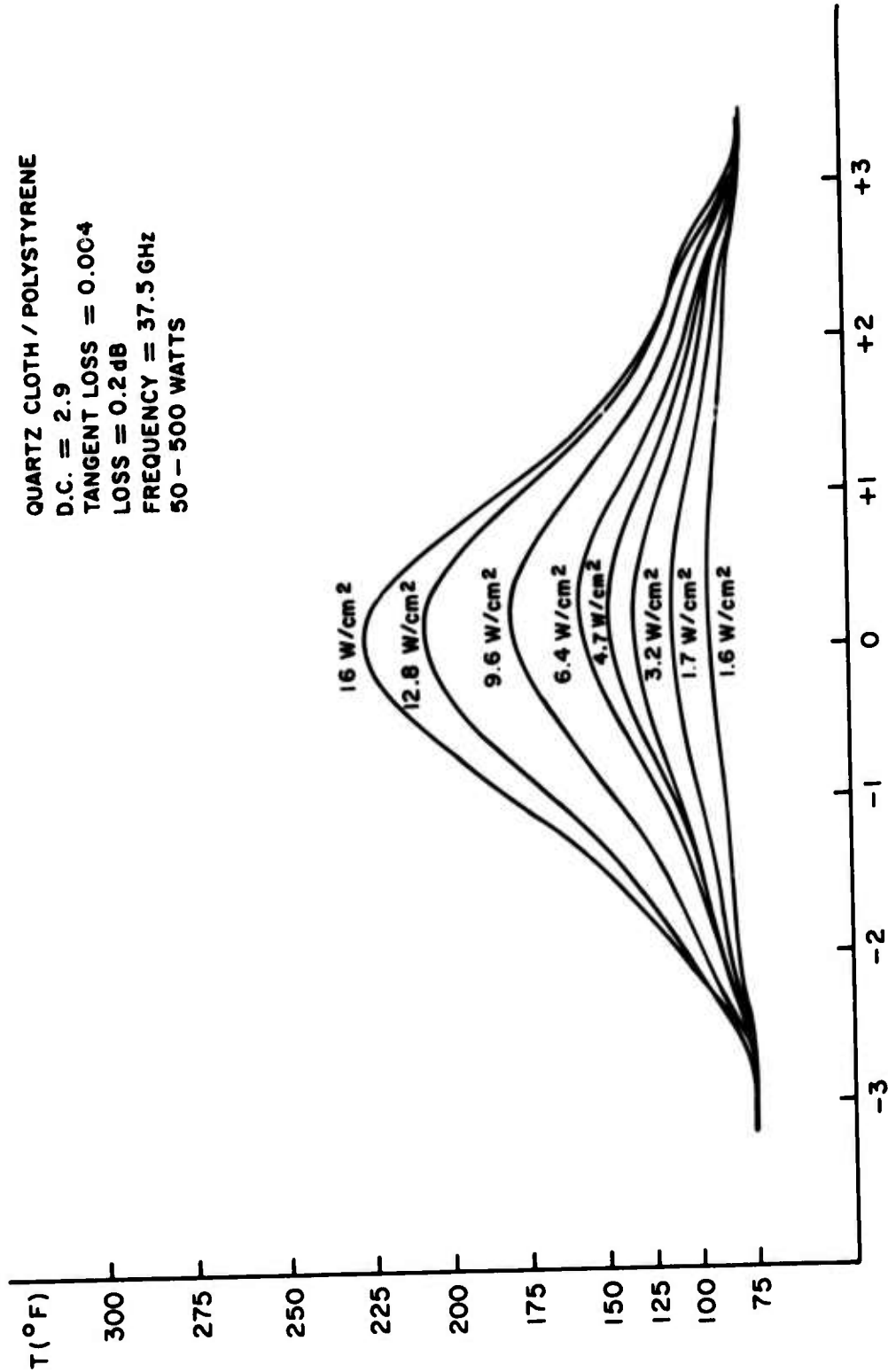


Fig. 13 — Quartz cloth/polystyrene resin temperature as a function of power density and displacement  
 DISPLACEMENT (INCHES)

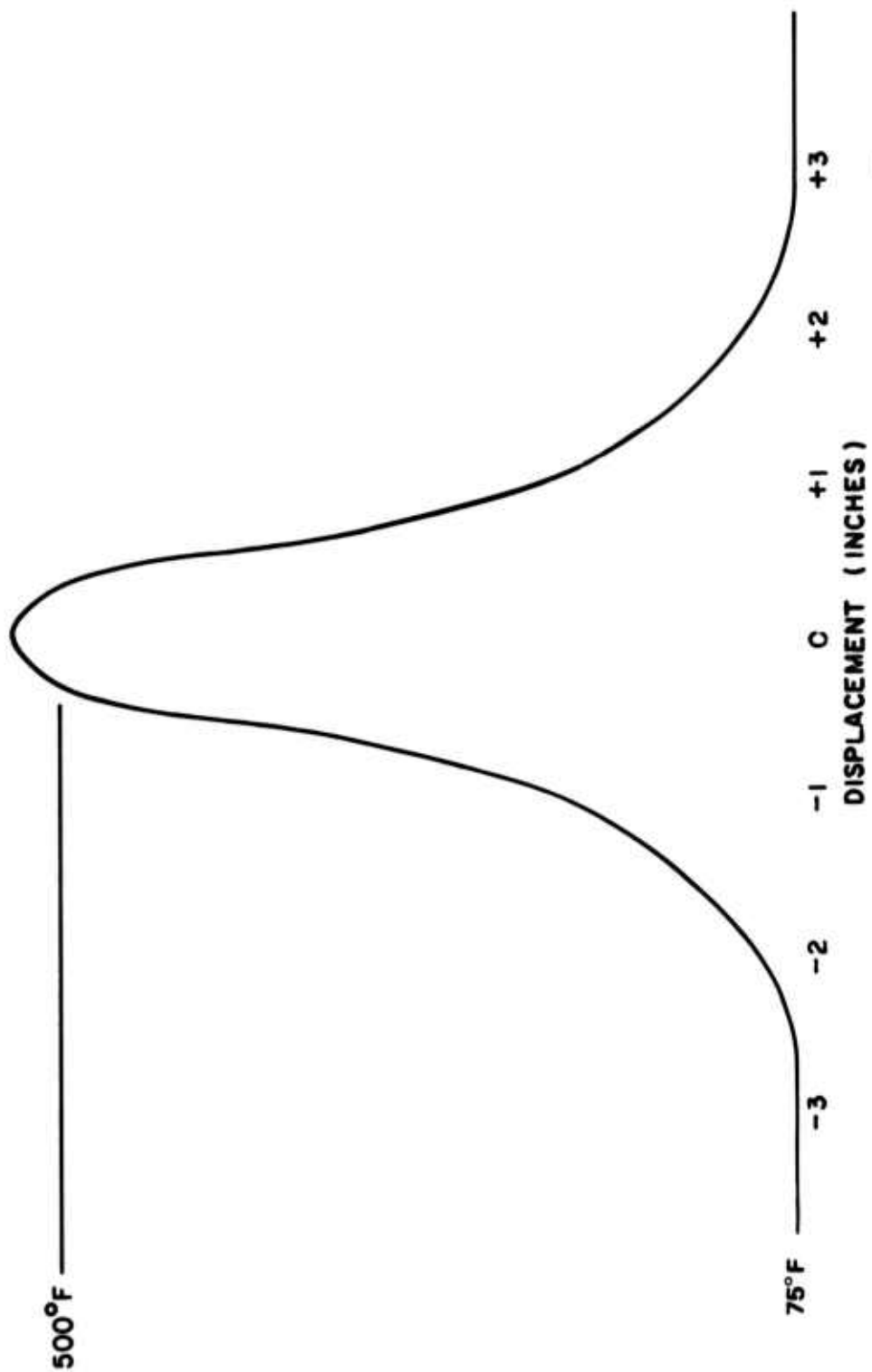


Fig. 14 — Type 326/7781 Dienite temperature as a function of displacement at 10 W/cm<sup>2</sup>

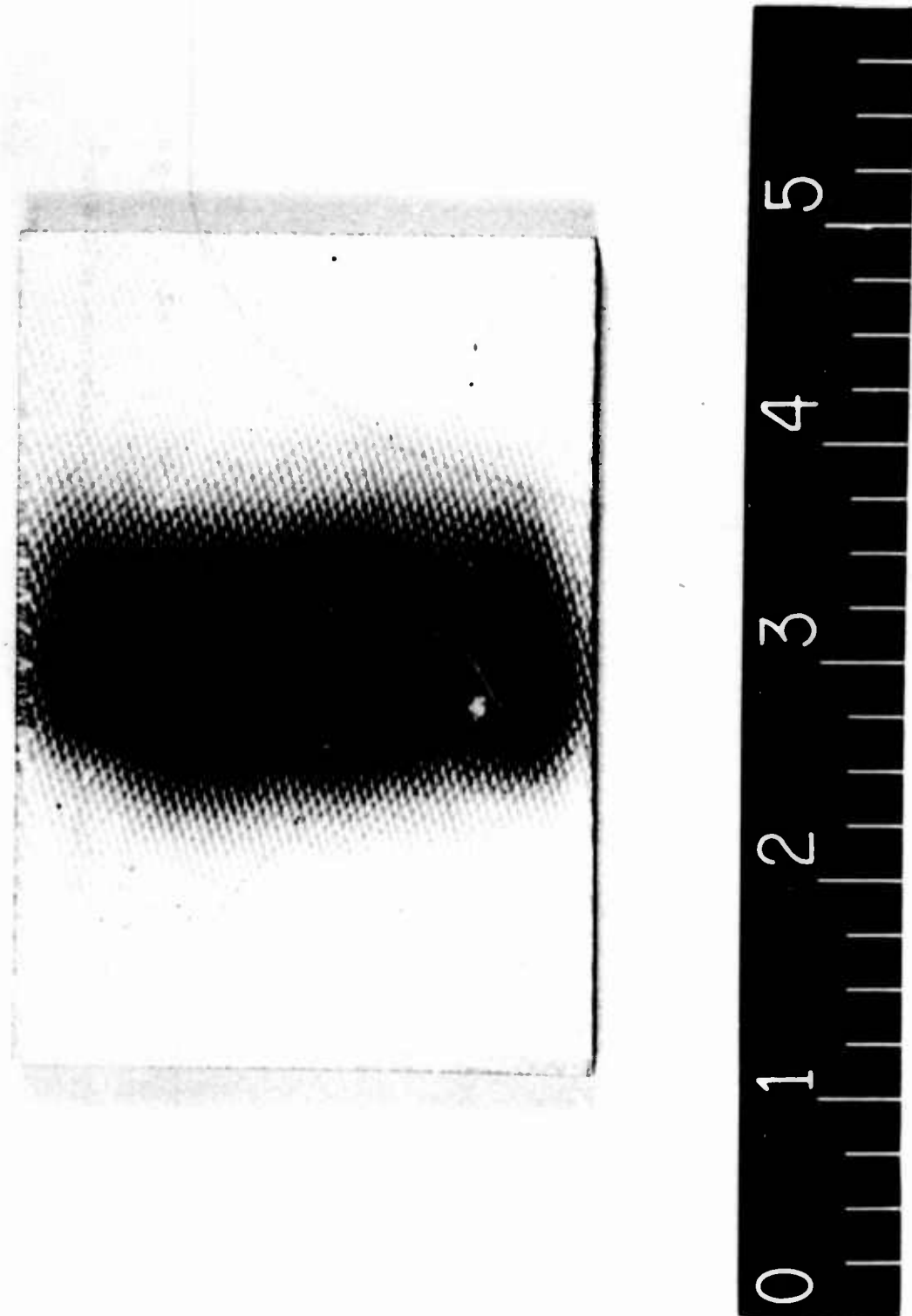


Fig. 15 — Type 326/7781 Dienite after being subjected to 10 W/cm<sup>2</sup> for 4 minutes



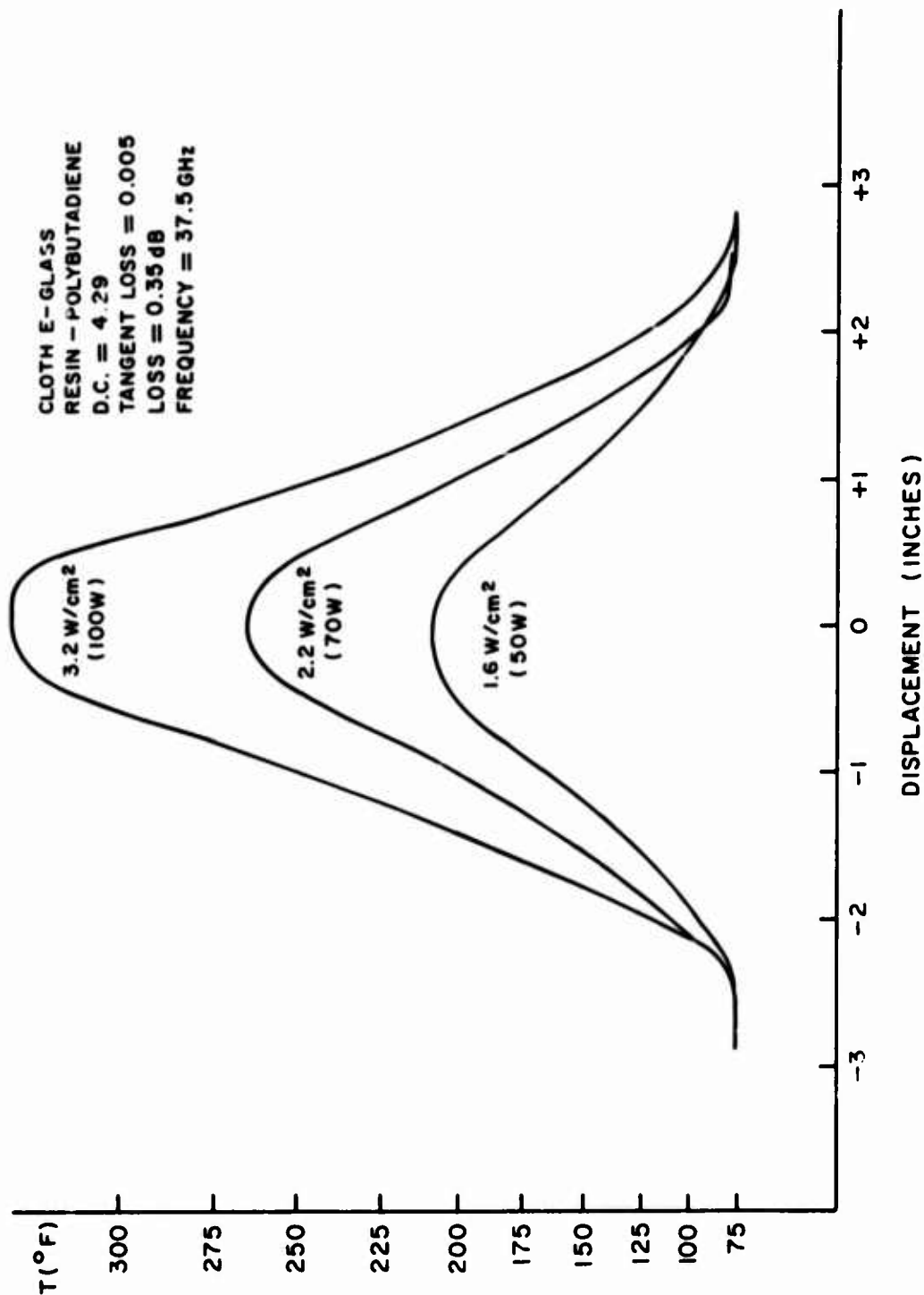


Fig. 16 -- Type U341 style 7781 E-glass/polybutadiene temperature vs power density and displacement

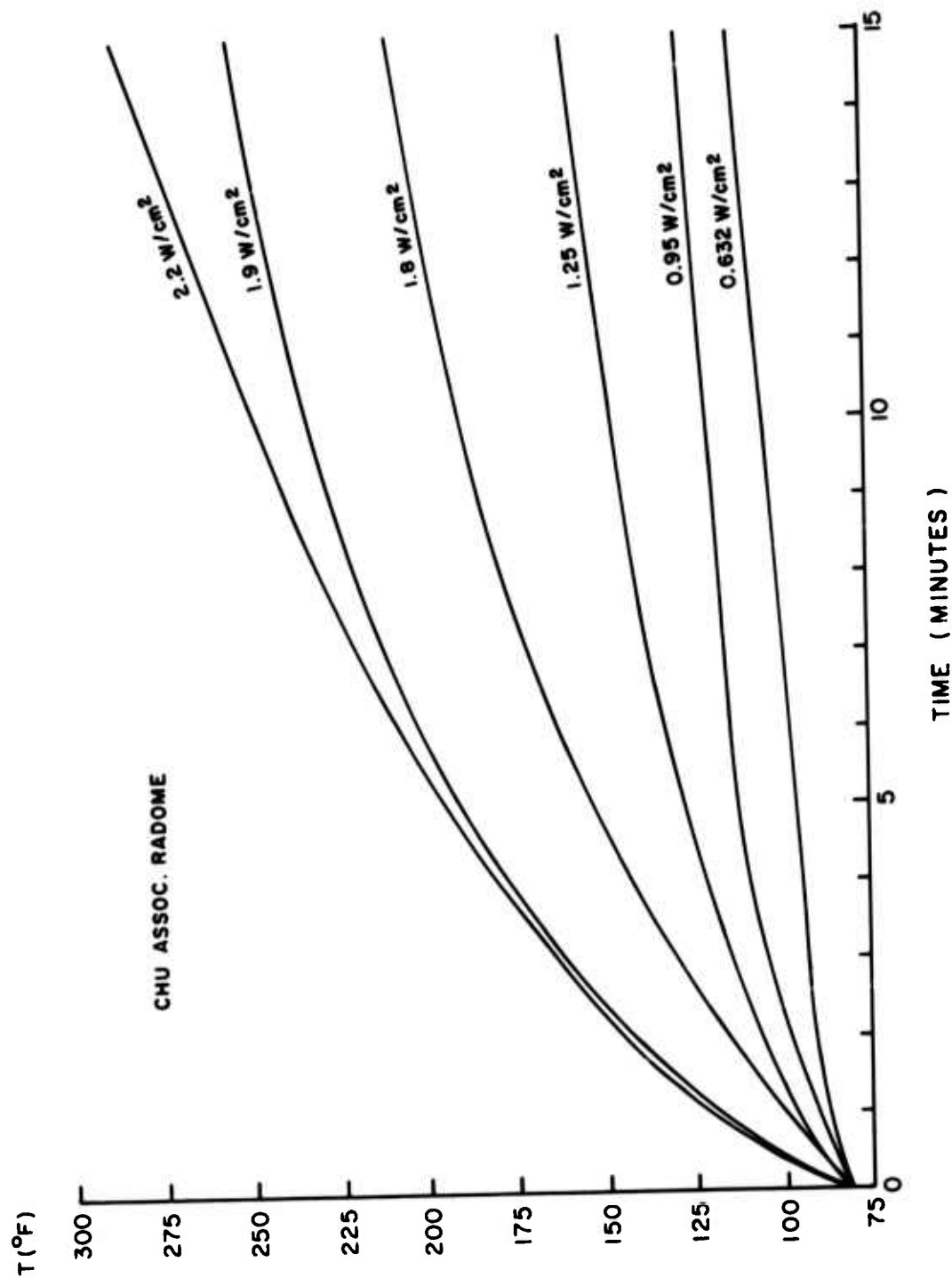


Fig. 17 — Temperature vs time characteristics of the NELC radome sample

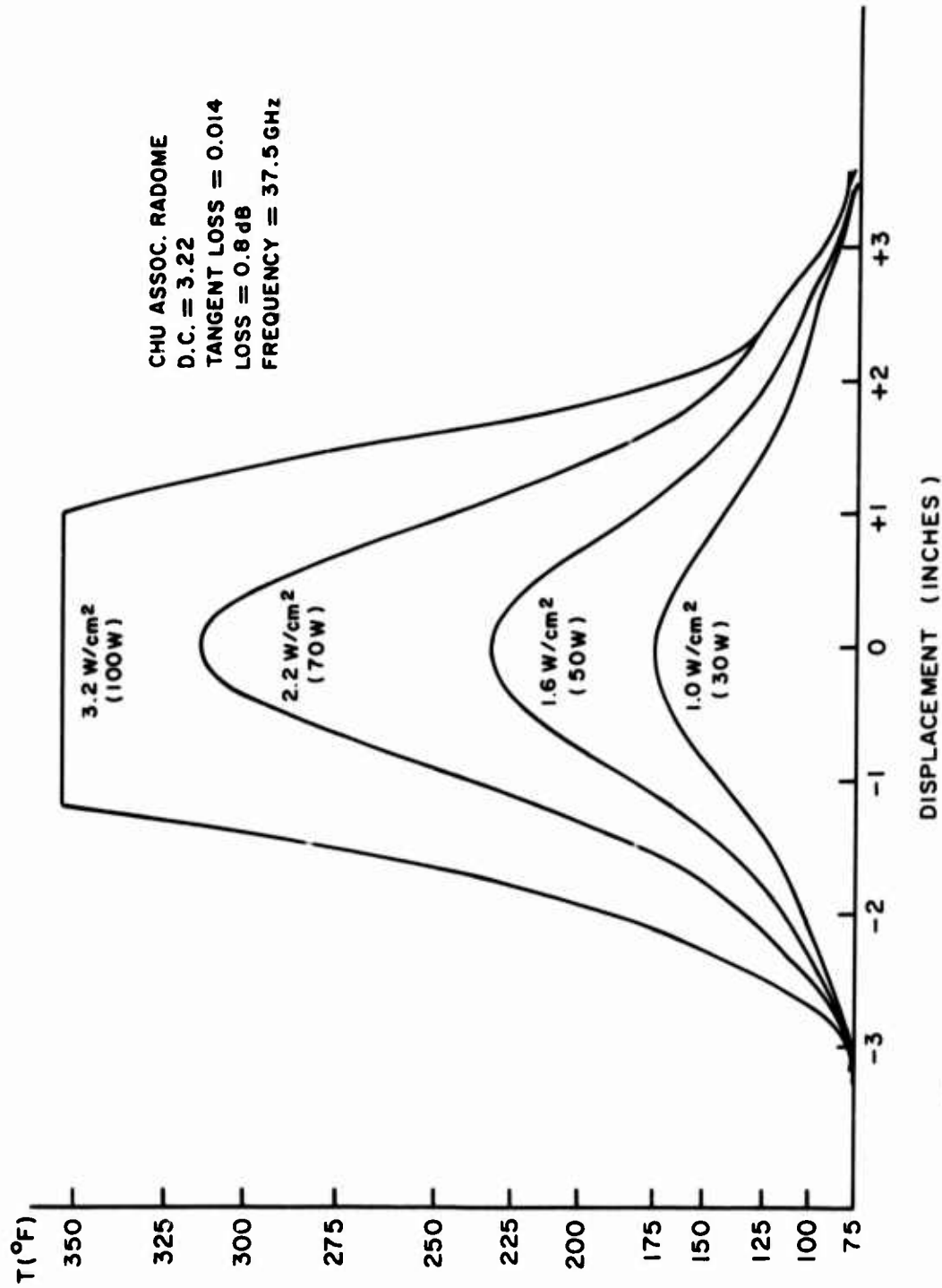


Fig. 18 — NELC radome sample temperature vs power density and displacement

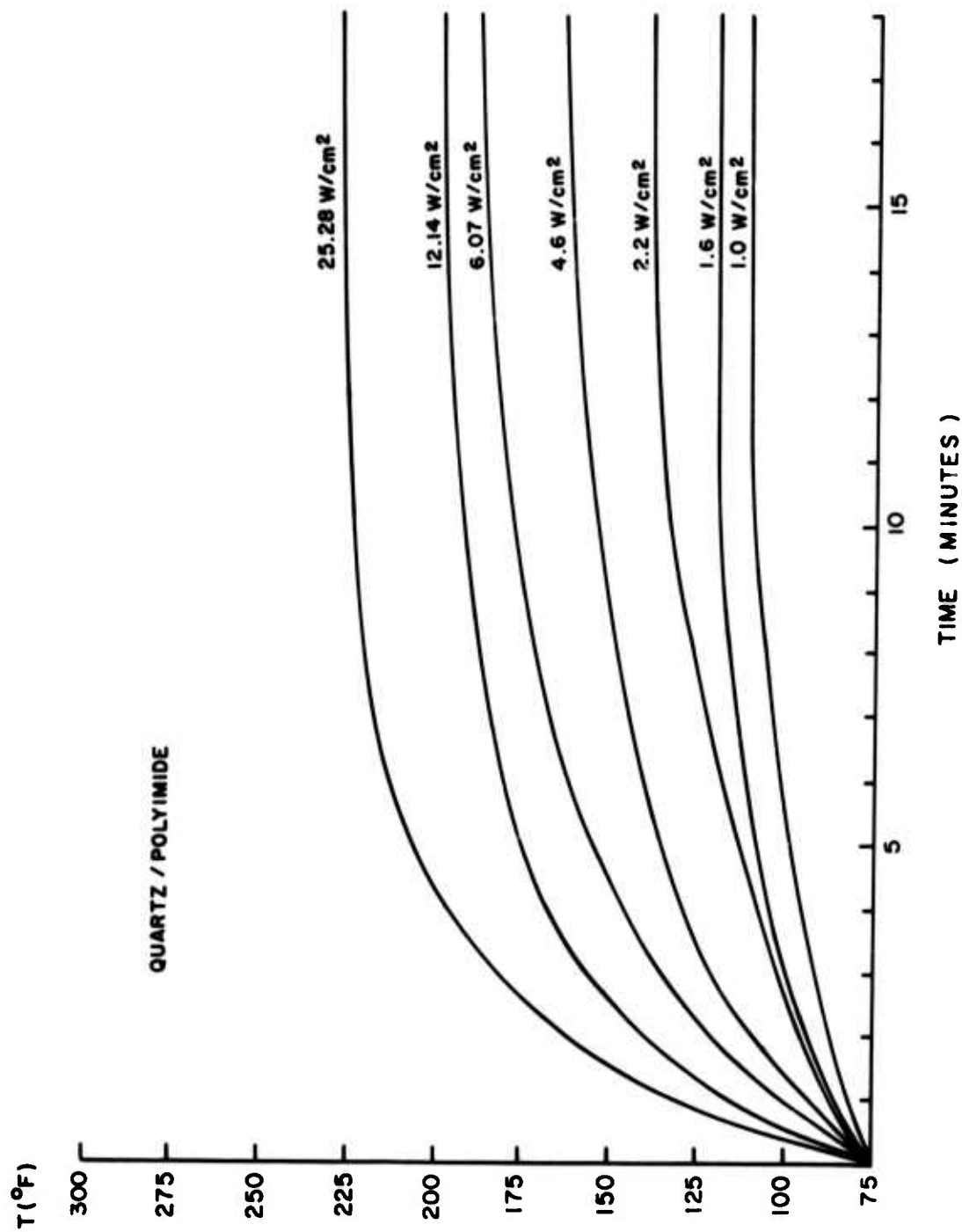


Fig. 19 — Quartz glass/polyimide resin temperature characteristics as a function of power density and time

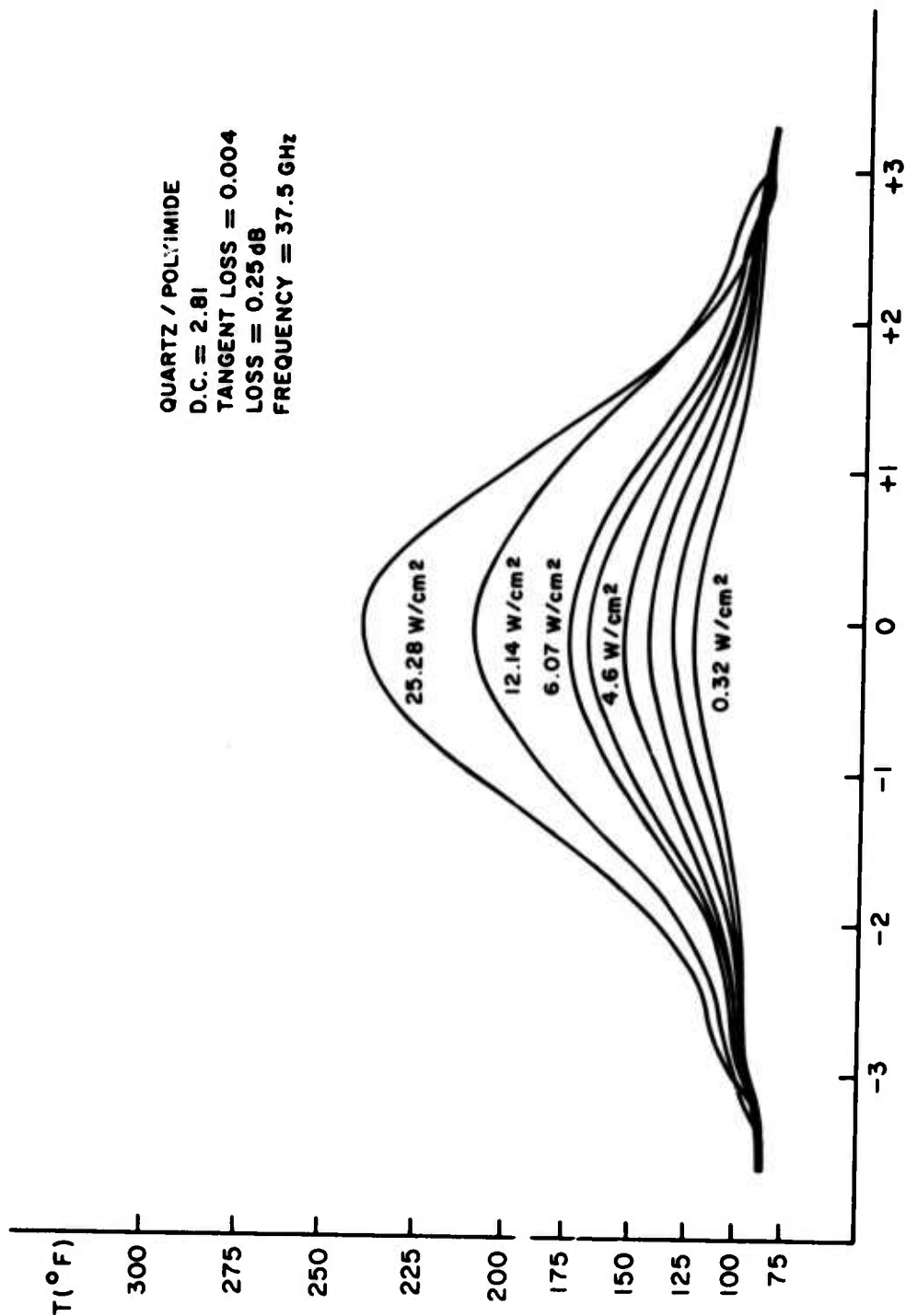


Fig. 20 -- Quartz glass/polyimide resin temperature as a function  
 of power density and displacement

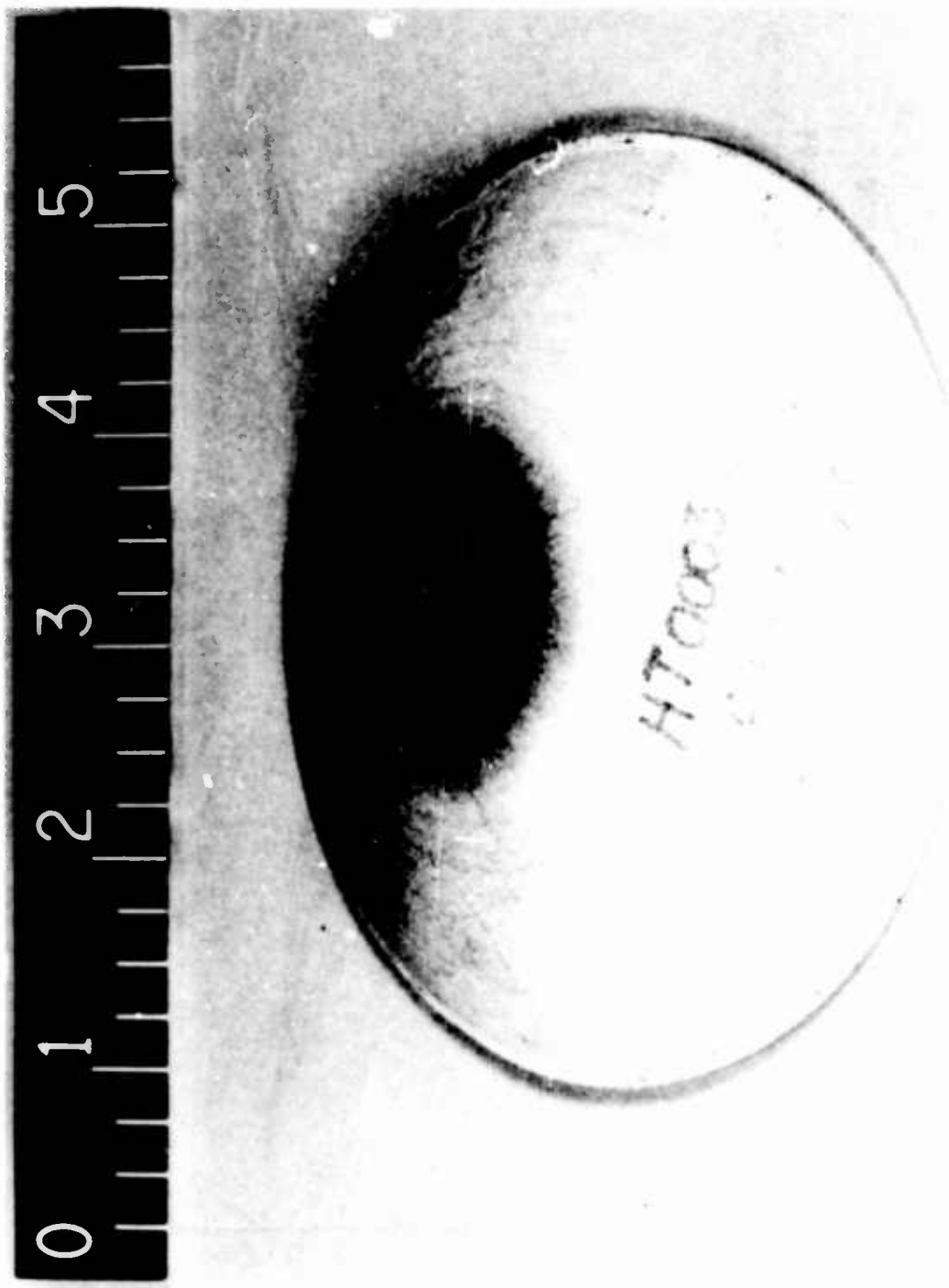


Fig. 21 — Original NRL lens dielectric after test



Fig. 22 — Cutaway view of original NRL lens after test